

## New Flow Features in a Cavity During Shock Wave Impact

B. W. Skews<sup>1</sup>, H. Kleine<sup>2</sup>, T. Barber<sup>3</sup> and M. Iannucelli<sup>4</sup>

<sup>1</sup>School of Mechanical, Industrial, and Aeronautical Engineering, University of the Witwatersrand, Johannesburg, 2050 SOUTH AFRICA

<sup>2</sup>School of Aerospace, Civil, and Mechanical Engineering, University of New South Wales, Australian Defence Force Academy, Canberra, ACT 2600 AUSTRALIA

<sup>3</sup>School of Mechanical and Manufacturing Engineering, University of New South Wales, Sydney, NSW 2052 AUSTRALIA

<sup>4</sup>Department of Mechanics and Aeronautics, University of Rome "La Sapienza", 18 - 00184 Rome, ITALY

### Abstract

Complex flows are induced in a cavity impacted by a shock wave. Early work concentrated on shallow parabolic cavities with the main interest being the focussing properties. Work on cylindrical surfaces has concentrated on wave reflection regimes. The advent of high framing rate, multi-frame, digital cameras has allowed much more detailed studies to be undertaken, which have identified a number of new features, as well as clarifying and modifying previous findings. Weak perturbations are introduced into the flow as identifiers of regions of influence from particular points on the wall. Particular emphasis is placed on the study of some new reflection patterns, the manner in which the waves focus in different cavity shapes, and complex shear layer flows with jetting and the development of Kelvin-Helmholtz instabilities.

### Introduction

Early studies of the impact of a shock wave on a cavity were primarily done using parabolic cavities with the primary purpose of establishing the peak pressures that could be generated due to focusing effects. The classic work is that of Sturtevant and Kulkarny [1], whose study concentrated on the trajectories of the triple points and the pressure variations in various parts of the cavity. Unfortunately the window through which they examined the flows did not cover the full height of the cavity, resulting in them missing some of the features which are currently being explored. Izumi et al. [2] compared experiment with simulation for a range of parabolic cavities of different depth to aperture ratios with the deepest one being for a ratio of unity. Different focusing types were identified depending on whether the reflected waves crossed on the symmetry plane before or after focus. Numerical resolution in these studies was insufficient to capture many of the details of the flow.

In the case of cylindrical cavities previous studies have concentrated on shock wave reflection off the surface and not on the focusing features which result when the shock is fully reflected from the base of the cavity. The majority of this work, mostly done by Ben-Dor and co-workers, is summarised in his monograph [3]. They concentrate on the transition from the initial Mach reflection (MR), formed when the shock enters the cavity, to Transitioned Regular Reflection (TRR) when the wall angle steepens and Mach reflection is no longer possible. These transitions will also be discussed in the current work.

A comprehensive study of the flow fields induced in a cylindrical cavity impacted by a shock wave has recently been conducted [4]. The overall interaction regime is indicated in Fig. 1, showing the patterns on one side of the plane of symmetry.

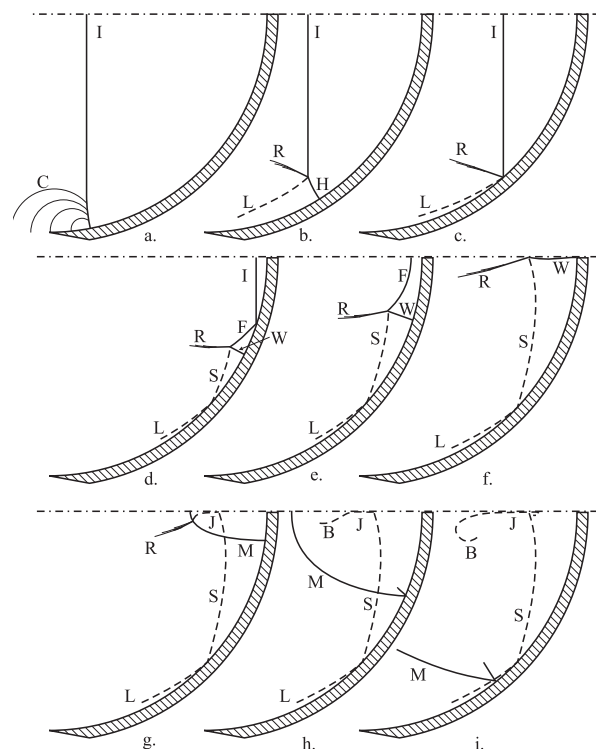


Figure 1: Schematic of the main features in a medium strength shock wave interaction with a cylindrical cavity.

At the entrance to the cavity the reflected wave consists of a fan of compression waves (C) which bend the base of the incident shock forward. These soon steepen up into a reflected shock (R) forming a Mach reflection with a Mach stem (H), and slipstream (L). Because of the steepening wall angle this becomes an inverse Mach reflection (Fig. 1c) and the triple point moves to the wall. This then becomes a Transitioned Regular Reflection, TRR, [3] (Fig. 1d). Here the incident wave reflects regularly off the wall with the new reflected wave (F) meeting the original reflected wave (R) in a new triple point with the third wave (W), termed the wall shock, connecting the triple point with the wall in order to balance the pressures. A new shear layer (S) is formed and the original shear layer (L) is left behind. Eventually the incident wave is fully reflected and the wave (F), now termed the focussing wave, develops into an imploding cylindrical wave.

The gas dynamic focus occurs when the reflected wave (R), the wall shock (W), and the shear layer (S) from either side of the cavity meet on the axis of symmetry (Fig. 1f). The two wall shocks merge to become the main reflected wave (M). It has perhaps not been previously appreciated that it is the wall shock of the TRR which develops into the main reflected wave. The two shear layers meet and combine to form a strong jet (J) facing towards the cavity entrance. The interaction of the main reflected wave with the original reflected waves (R) results in new triple points and shear layers (B). The waves (R) are totally overtaken, the shear layers are left behind, and the main reflected wave becomes smooth. At the same time the jet pushes in between the shear layers (B) causing them to roll up into vortices. Where the two TRR shear layers meet a small opposing jet facing in the opposite direction to the main jet is developed. One of the most interesting features of the subsequent motion is the development of strong Kelvin-Helmholtz instabilities on the shear layers. The complex jet and shear layer behaviour are shown in Fig. 2, and are dealt with more fully in [4].

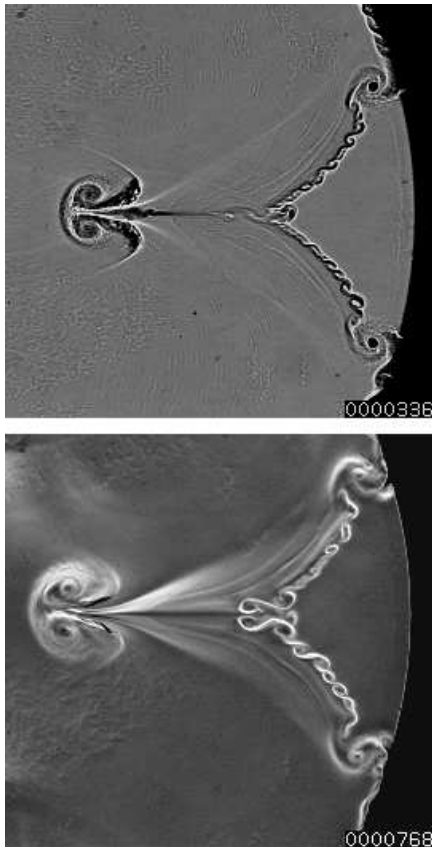


Figure 2: A shadow and schlieren image of the jets and instabilities associated with the shear layers.

### Experimental Arrangement

Experiments were conducted in a shock tube with a test section 150 mm high and 75 mm deep. A 10 mm gap was left between the test piece and the top and bottom of the tube. Three experimental models are dealt with in this paper: the circular arc case described above, a parabolic surface of the same depth (65 mm) and aperture (130 mm) as the circular reflector, and a deep parabola nearly twice as deep (126 mm). Imaging was done with a Shimadzu high-speed camera, having the facility to take 102 full frames at rates of up to one million per second.

The flow was observed by means of shadowgraph and omnidirectional (circular cutoff) schlieren visualisation. In some tests strips of 45 micron thick tape were attached transversely at intervals on the wall of the cavity to generate weak perturbations, thereby supplying a tracer of how signals from the wall influence the interior of the flow [5].

### Wall Reflection

Early work on the reflection from a cylindrical cavity suggested that Mach reflection was initiated as the wave engaged with the entrance [3]. It is shown in [4] that this is not so and that a compression wave first develops which causes a kink in the shock which in turn develops into a triple point. However, the important point is that the initial corner signal impacts the shock higher up than where the triple point develops. Thus the incident shock is already curved above the triple point and the reflected shock appears to terminate in space as it blends with the dispersed compression. In the case of a parabola, however, since there is a finite wall angle at the entrance of the cavity, the Mach reflection does develop immediately with a finite strength reflected shock, which will be referred to as the lip shock.

### Weak Incident Wave Reflection

For weak shocks the situation is somewhat less clear than indicated in Fig. 1. Figure 3 shows images from two tests, the upper one with shadowgraph and the other with schlieren, of Mach 1.04 shocks reflecting off the cylindrical surface. Whether the reflection is initially regular, as appears to be the case in the shadowgraph, is uncertain. The corner signal intersects the shock higher up the shock and is barely discernible in the original image because of the very weak incident shock. The resolution is also insufficient to clearly see the formation of the reflected shock. However, what is clear in the images taken 70  $\mu$ s later is a pattern somewhat different from a TRR. No slipstream can be detected and the reflection may be more in the nature of a von Neumann Reflection (vNR). The schlieren images show a rather non-uniform region behind the interaction with indications of a complex density distribution. This region needs further investigation.

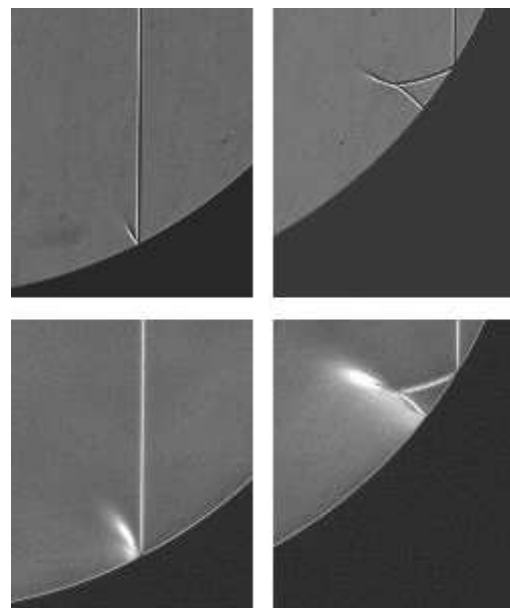


Figure 3: A pair each of shadowgraph and schlieren images of a Mach 1.04 shock reflection. 70  $\mu$ s between frames

This newly observed reflection pattern is also evident in reflection from a parabolic surface. Figure 4 is an image taken just before the incident shock strikes the back of the cavity. The weak perturbations from tape on the wall are clearly visible. It is clear that an exceptionally sensitive schlieren system is required to pick up these waves, which must be considerably weaker than the main waves. Nonetheless there is no sign of a shear layer arising from where the three main waves meet, although there are indications of strong gradients at the confluence. The slope of the lip shock and focussing shock appear to be continuous, again suggesting a von Neumann reflection.

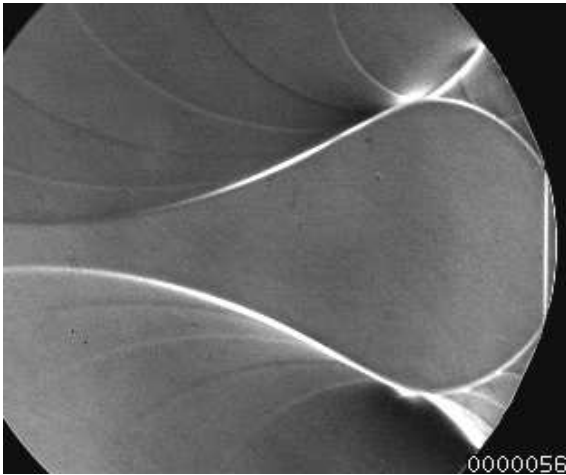


Figure 4: Schlieren image of a Mach 1.03 shock wave reflecting in the shallow parabolic cavity

It is also interesting how the wall perturbations coming off the thin transverse wall tapes give an impression of a relief pattern with alternate light and dark lines. These result from alternate compression and expansion waves being produced as the incident wave passes over the edges of the tape, first as it rises over the leading edge followed by it passing over the trailing edge of each strip of tape. These waves meet the lip shocks at a small angle thus giving a further indication of the weakness of this wave, as shown in [5].

#### **Stronger Wave Reflection**

The topography of the cylindrical and shallow parabola reflections are similar, but that of the deep parabola is strikingly different. The top two images of Fig. 5 are for the cylinder and shallow parabola respectively, whereas the two below are for the deep parabola. The latter images are at a magnified scale. In the top two the progression is from MR to TRR, the main difference being that for the cylinder there is a weak corner signal but for the parabola there is a strong reflected lip shock. For the deep cavity the lip shocks from either side cross each other forming a triple point with the incident shock and a large Mach stem. However, the reflection is not a conventional Mach reflection as there is no shear layer and the incident wave and the stem have a smoothly varying tangent, again indicating a von Neumann type reflection. What is very noticeable, however, is the marked curvature of the stem as it approaches the wall. The situation becomes similar to that at entrance to the cylindrical cavity with the development of a kink in the shock as the compression waves from the increasing slope of the wall merge to eventually cause a Mach reflection, with its associated slipstream, as is evident in Fig. 5d. The base of the stem continually increases in strength and interacts with the slight roughnesses on the surface of the test piece producing clearly

visible perturbations, in spite of a fine surface finish of the test piece. This case is also interesting from the point of view that the two triple points on the lip shock will meet very close to the base of the cavity totally engulfing the plane incident wave. This means that the wave will be curved along its entire length before it is fully reflected. Further tests will be necessary to establish the influence of the cross over of the lip shock, not only on the reflection pattern, but on the subsequent motion.

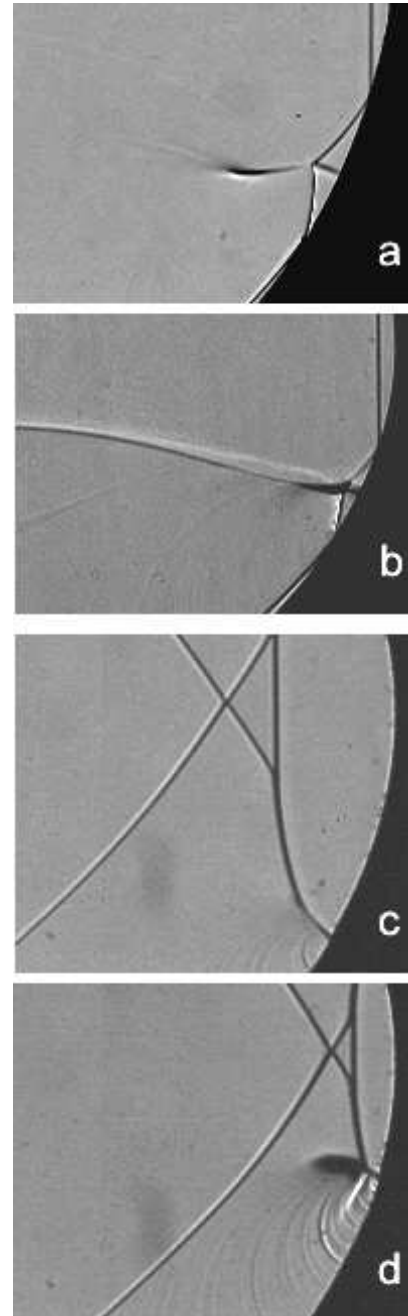


Figure 5: Shadow images of Mach 1.23 shock wave reflection on: a) cylindrical, b) shallow parabolic, and c,d) deep parabolic, cavities

#### **Focus and Post-focus evolution**

As in the case of reflection the focussing process will depend on both the Mach number and the cavity shape.

### The Weak Wave Case

Figure 6 shows flow patterns for a Mach 1.03 wave for the three cavities under focus and post-focus conditions. In the cylindrical case the test was conducted with the wall tapes in place. Although the perturbations are very weak, except for the lip wave because of the blunt model entry, it can be discerned that the first four perturbations bypass the focal point entirely whereas the later ones converge in the formation of the small reflected shocks. This is in contrast to the shallow parabola where the lip and wall shocks all meet at a point. The slight perturbations in the bright area around the focal point also indicate a converging flow. This is to be expected for a parabolic cavity with a near-acoustic wave. However, the deeper parabola again shows a different behaviour. No clear focus is visible since the wall shocks do not converge to the same point as the lip shocks. The reflected waves from the original Mach reflection are also still visible, indicating that the compressions from the wall are not concentrating to a point.

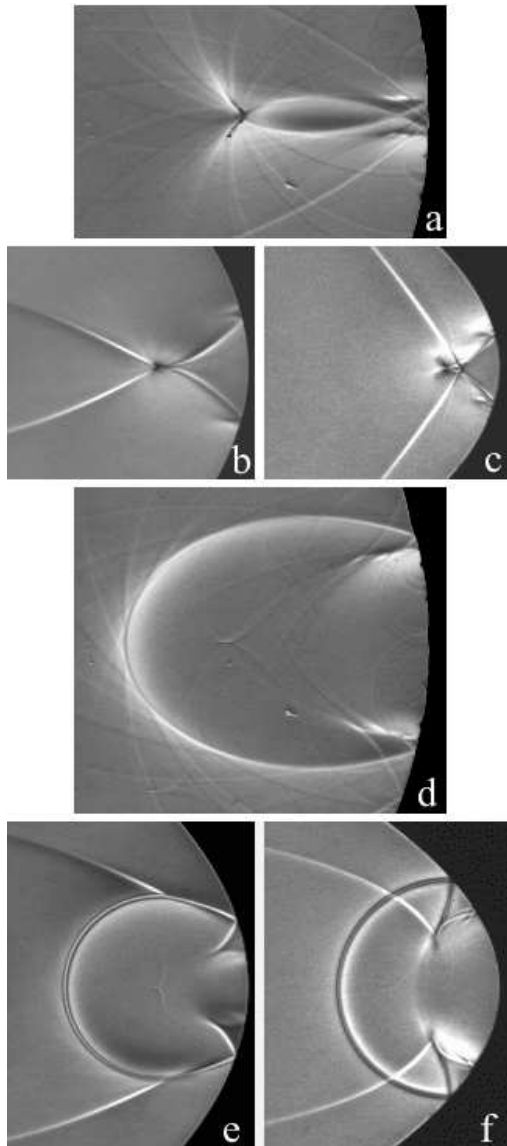


Figure 6: Schlieren images of focus (top three images), and 40  $\mu$ s post-focus (bottom three images) of a Mach 1.03 shock impinging on a cylindrical (a,d), shallow parabolic (b,e) and deep parabolic (c,f) cavities

The post-focus flow is similar for all cavities in that a smooth main reflected shock is formed. There are, however, some significant differences between the two parabolic cavities: in the shallow case the lip shock merges with the main reflected shock without a visible slipstream and again suggesting a von Neumann type reflection, whereas in the deep case it passes right through. Furthermore, it is noted in the centre of the first two post-focus images (Fig. 6 d and e) there is evidence of a typical TRR shear layer, meeting in a slightly brighter spot. It is barely visible in the third image (Fig. 6 f) but again becomes clearer for this cavity for a Mach 1.05 shock. The interesting point is that there is no evidence of these layers during the earlier reflection from the wall (Figs. 3 and 4). It would thus appear that what starts out as a weak reflection, without a detectable slipstream, transforms into a conventional Mach reflection as the wall shock gets stronger and the angle between the waves change. The shear layer would thus be generated only part way through the motion. High resolution simulations will become necessary to explore the evolution of these systems in more detail. It is also noted that the main reflected wave meets the cavity wall at an angle thereby generating a regular reflection followed by a further wave.

### Stronger Wave Case

With stronger incident waves many of the post-focus features become more marked as shown in Fig. 7. Particularly noticeable is the growth of the shear layer arising from the TRR and the jet that develops [4]. Unlike for the weaker case shown in Fig. 6 the jet bifurcates due to the development of new three-shock intersections resulting from the overtaking of the reflected waves arising from the initial Mach reflection, by the main reflected wave formed from the wall shocks. However, because of their limited extent these waves are overtaken and the main reflected wave becomes smooth, as occurs for the weaker wave case.

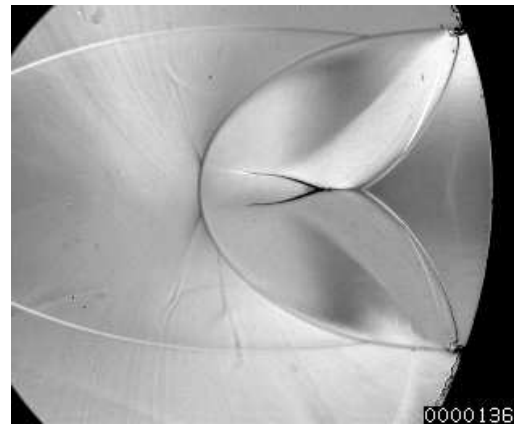


Figure 7: Post-focus flow patterns for a strong  $M=1.33$  incident wave on a cylindrical cavity

The evidence of flow non-linearity is also more apparent for the stronger shock waves. Cases for the three cavities are given in Fig. 8, the first two with perturbations made visible with the wall tape and the third with them arising from wall roughness. In the cylindrical case the wall perturbations do not contribute directly to the formation of the focus, as in the case of the weak shock (Fig. 6) but bunch together to form the reflected shocks which then meet, together with the wall shock on the axis of symmetry. The contrast between the weak and strong shock case is more dramatic for the shallow parabolic cavity. For the strong shock the perturbations blend in with the finite lip shock strengthening it, and causing it to turn towards the axis of sym-

metry. The deep parabola again gives a different result because the lip shock has already reflected off the base of the cavity, and the compression from the wall, as shown by the perturbations, form a new reflected shock system.

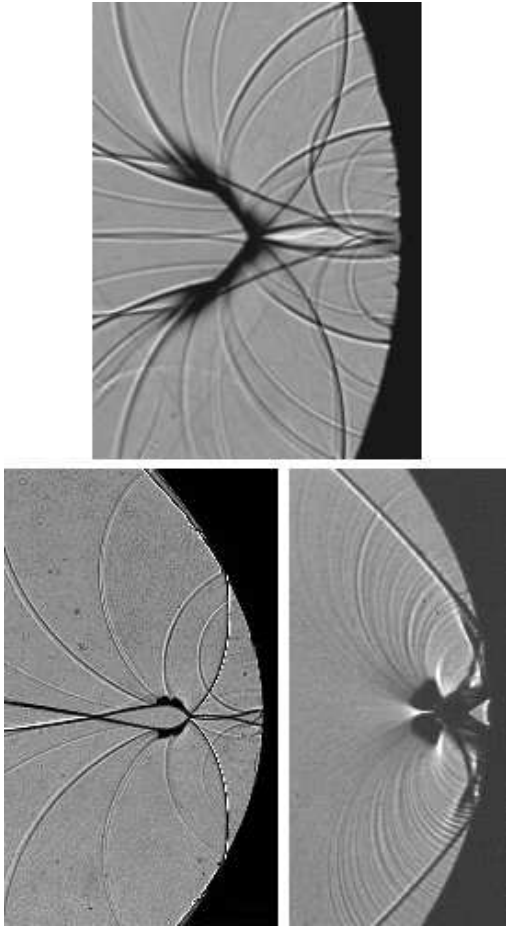


Figure 8: Shadow images of focus of a Mach 1.23 shock impinging on a cylindrical (top), shallow parabolic (bottom left) and deep parabolic (bottom right) cavities

### Shear Layer Development

The major point of interest in the post-focus situation is in the growth and development of the shear layers. Figure 2 shows the very interesting flow patterns that are generated in the cylindrical cavity. These are contrasted in Fig. 9 for the other two cases. For the shallow parabola the pattern is similar to that for the cylinder except that in view of the finite strength of the lip shock its interaction with the main reflected wave causes a three-shock intersection with the associated shear layer. Thus rather than the shear layer being stranded it continues to be generated outwards. The first image of the bottom pair is for the same test but taken 200  $\mu$ s later. The forward facing jet pulls the new shear layers forward and all the layers develop KH instabilities at various positions, including the original one adjacent to the wall.

The images for the deep cavity (middle and bottom right images) are from two different tests taken at different magnifications in order to obtain some detail of the jet in this case. It is clearly somewhat different from the previous case, primarily because the reflection process is so different (Fig. 5). There are two very marked shear layers adjacent to the wall resulting from

the highly curved Mach stem generated earlier breaking into a new Mach reflection. The jet also pushes forward into the layers that develop from the intersection of the lip shock with the main reflected wave as in the case for the shallow parabola. However, as the lip shock is developed much earlier due to greater cavity depth the shear layers cross over each other as shown in the middle image. The intersection between the lip shock and the main reflected wave results in new truncated reflected waves being generated.

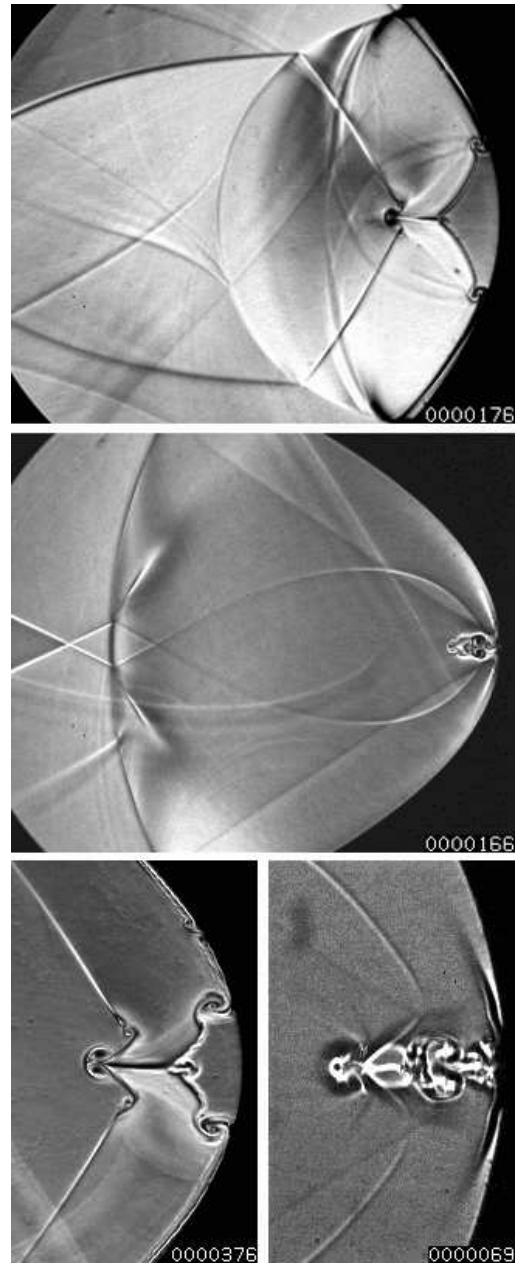


Figure 9: Shear layer and jet development. Top: Shallow cavity,  $M=1.34$ . Middle: Deep cavity,  $M=1.23$ . Lower two images show corresponding shear layer behaviour in more detail.

### Preliminary Simulation results

Computational Fluid Dynamics has been used to attempt to capture the major features found in the experimental results. In these preliminary results, a cylindrical cavity at  $M=1.24$  has

been simulated. The Fluent solver has been used to solve the equations and the solutions were run on the ac3 supercomputing cluster, which is a facility jointly owned by the NSW State Government and a number of NSW Universities.

A structured mesh of approximately 1.8 million structured elements is used, with a symmetry boundary condition at the horizontal centreline. In order to study the effect that this constraint may have on the flow features, a full two-dimensional mesh was solved. No variation was found from the symmetric solutions. The solutions were solved with a pressure-based solver, and varying levels of equations discretisation were used. Originally a 3rd order MUSCL scheme was used for all equations, however 2nd order and bounded central differencing schemes were also utilised in an attempt to capture the post-focus shear layer development. Pressure-velocity coupling was via the PISO algorithm. Timesteps were generally  $0.001\mu s$ .

### Pre-focus Feature Resolution

The main features of the cylindrical cavity shock reflection have been resolved well. Figures 10 and 11 should be compared with Figs. 1b and 1e. The fan of compression waves begins at the base of the cavity, developing into the reflected shock, as seen in Fig. 10. The Mach stem (H in Fig. 1b) and slipstream (L) are easily located in the numerical solution

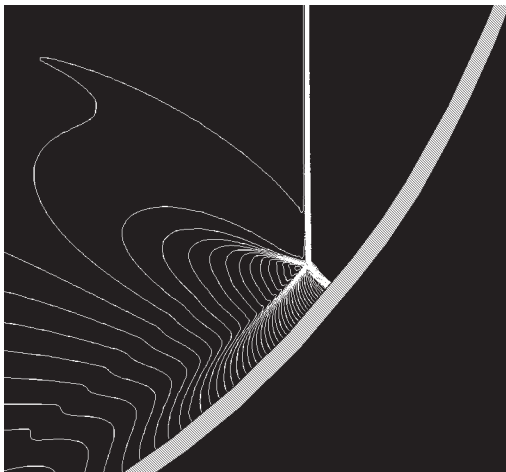


Figure 10: Numerical solution of  $M=1.24$  cylindrical cavity, demonstrating the development of the Mach stem and slipstream. Density contours are displayed to provide visualisation of the flow features. This image should be compared with Fig. 1b.

In Fig. 11 the flow features shortly after formation of the TRR are presented. The reflected shock (R) is seen to intersect with the new reflected wave (F) and the third wave (W) and the development of the new shear layer is also clearly visible. A small vortex is apparent where the shear layer meets the wall.

### Post-focus Feature Resolution

For the post-focus behaviour, the shock interaction is reasonably predicted but the shear layer behaviour is not well-resolved. Figure 12 shows the flow development shortly after the focus, and the converging of the reflected wave, wall shock and shear layer is seen. The two wall shocks are now merging to form the main reflected wave (M in Fig. 1). The original shear layer is still clearly visible, with a vortex which has formed at the wall intersection. This vortex formation and its subsequent movement are critical to the later development of the jets and

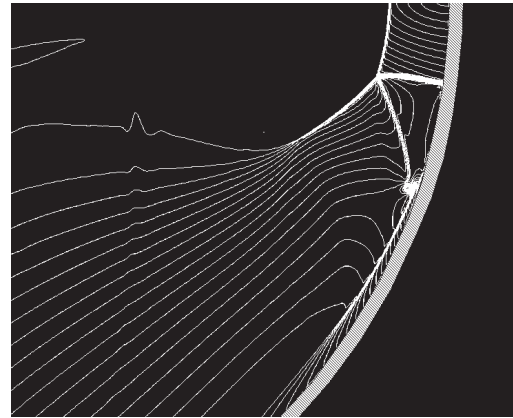


Figure 11: Numerical solution of  $M=1.24$  cylindrical cavity, demonstrating the development of the new shear layer. Density contours are displayed to provide visualisation of the flow features. This image should be compared with Fig. 1e.

instabilities seen in the experimental work.

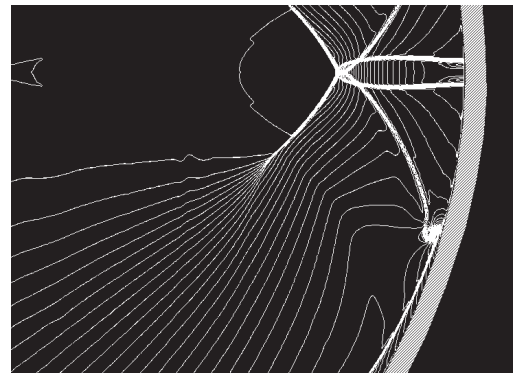


Figure 12: Numerical solution of  $M=1.24$  cylindrical cavity, shortly after the focus. Density contours are displayed to provide visualisation of the flow features.

The strong main reflected wave is shown in Fig. 13, where the post-focus flow patterns are displayed. The weaker lip shock can also be seen, extending towards the cavity inlet from the lower section of the main reflected wave. Evidence of the formation of a jet is apparent along the centerline of the cavity and the overall features are similar to those seen for the experimental  $M=1.33$  case, shown in Fig. 7.

Further development of the jet in the numerical solution becomes less similar to the experimental results. While a large roll-up region is seen at the cavity wall, it moves further towards the symmetry plane than is seen experimentally, and the shear layer instabilities found in the experimental results are not visible. The overall structure is similar to that found in the schlieren images, however, the features seen, for example in Fig. 2, are not evident in the numerical images.

Work is continuing in this area, with an emphasis on developing an appropriate methodology to capture the shear layer instabilities. Viscosity has been introduced into the equations without any significant variation in the results, however it is possible that the already fine mesh may need further refinement in the region of the wall boundary layer. Also, a means by which to introduce an asymmetric disturbance is being investigated, as this may be required to initiate the instability. A non-symmetric, full 2D



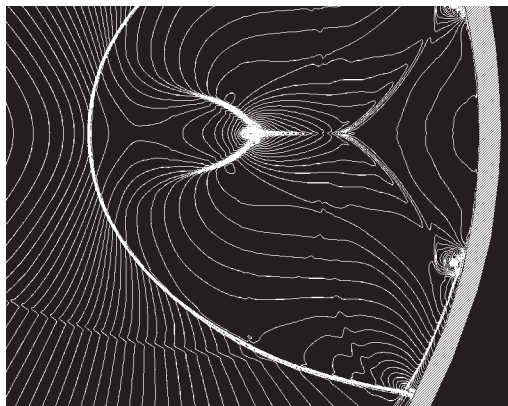


Figure 13: Numerical solution of  $M=1.24$  cylindrical cavity, demonstrating the post-focus flow patterns. Density contours are displayed to provide visualisation of the flow features.

mesh (with regions away from the wall containing unstructured elements to allow for numerical asymmetry in the solution) has been used as one method to attain this disturbance. While the results did indeed show an asymmetric instability arising, the formation of the wall vortices was still not accurately resolved.

### Conclusions

A detailed study of the interaction of a shock wave with a variety of cavity shapes has identified a number of new interaction patterns which can be strongly influenced by both cavity shape and shock Mach number, resulting in a wide variety of flow features. The present work has concentrated on a phenomenological description of these features but has also highlighted the need for further, more quantitative investigations. Time-resolved visualisation has clarified the evolution of the flow patterns and revealed the role that the observed flow features play, but some processes have not yet been fully resolved. The nature of some observed reflection patterns remains to be clarified. Future experiments and simulations are planned to answer the new questions that have become apparent in this investigation.

### Acknowledgements

The support of the first author through a Rector's Fellowship to conduct research at ADFA is gratefully acknowledged.

### References

- [1] Sturtevant, B. and Kulkarny, V.A., The focusing of weak shock waves, *J. Fluid Mech.* **73**, 1976, 651–671.
- [2] Izumi, K., Aso, S. and Nishida, M., Experimental and computational studies focusing processes of shock waves reflected from parabolic reflectors. *Shock Waves* **3**, 1994, 213–222.
- [3] Ben-Dor, G., *Shock Wave Reflection Phenomena*, Springer, 1992.
- [4] Skews, B.W. and Kleine, H., Flow features resulting from shock wave impact on a cylindrical cavity, *J. Fluid Mech.* **580**, 2007, 481–493.
- [5] Skews, B.W. and Kleine, H., The use of weak waves as diagnostic tracers in unsteady flows, *5th Int. Conf. on Heat Transfer, Fluid Mechanics and Thermodynamics. HEFAT 2007*, editor J.P. Meyer, ISBN 978-1-86854-6435.